

Spectroscopy of nanosized composites consisting of silicon-organic polymers in nanoporous silicas

著者	SUTO Shozo, Ostapenko N., Kozlova N., Watanabe A.
journal or publication title	Low temperature physics
volume	32
number	11
page range	1035-1041
year	2006
URL	http://hdl.handle.net/10097/35051

doi: 10.1063/1.2389010

Spectroscopy of nanosized composites consisting of silicon-organic polymers in nanoporous silicas

N. Ostapenko^{a)} and N. Kozlova

Institute of Physics, National Academy of Science of Ukraine, 46 Nauka Ave., Kiev 03028, Ukraine

S. Suto

Department of Physics, Graduate School of Science, Tohoku University, Sendai 980-8578, Japan

A. Watanabe

Institute of Multidisciplinary Resource for Advanced Materials, Tohoku University, Sendai 980-8577, Japan
(Submitted May 15, 2006)

Fiz. Nizk. Temp. **32**, 1363–1371 (November 2006)

Fluorescence and excitation spectra ($T=5-290$ K) of nanosized silicon-organic polymers poly(di-*n*-hexylsilane) and poly(methyl(phenyl)silane) incorporated into porous silica materials MCM-41 and SBA-15 have been studied with varying pore diameter from 2.8 to 10 nm. The controlled variation of the pore diameter in a wide range (2.8–10 nm) permitted us, for the first time, to investigate the optical properties of the polymers on their transition from isolated macromolecules to a film. It is found that this transition depends on polymer type and occurs via the formation of new spatially independent structures of the polymers not observed in the spectra of the film, namely, via the formation of disordered and (or) ordered conformations of polymer chains and clusters. © 2006 American Institute of Physics. [DOI: [10.1063/1.2389010](https://doi.org/10.1063/1.2389010)]

INTRODUCTION

Wide application of nanosized polymers in different technologies such as transport and luminescent layers in electroluminescent diodes, sensors, and photoresistors^{1,2} stimulates the investigation of their optical and electrical properties. One of the promising methods of preparing nanosized polymers is nanocomposites of a “host-guest” type where a polymer (“guest”) is incorporated into nanopores of silica materials MCM-41 and SBA-15 (“host”). Varying nanopore size and composite composition makes it possible to change both the phase state and the structure of the nanostructure, many of its properties being changed compared to those of polymer films (luminescence efficiency, charge carrier mobility, diffusion coefficients of excited states, etc.). Controlling the nanocomposite structure enables one to exert control over their properties and to obtain new materials with prescribed characteristics.

The silicon-organic polymers are disordered media with weak intermolecular interactions between macromolecules. If the polymer is in a limited space, then the interactions between macromolecules and pore surface are of great importance in addition to the intermolecular ones. Controlling the variation of pore diameter over a wide range makes it possible to change the contribution of these interactions. If there is only an isolated macromolecule in a pore, the polymer surface interaction will be most important. It is this interaction in a pore of small diameter that is mainly responsible for the origination of new polymer states in composites.^{3–5} As the pore diameter increases, the number of polymer chains in the pore increases, too, and their microscopic properties may be quite different due to the modification of their conformation, packing and orientation.

We prepared nanocomposites based on silicon-organic polymers poly(di-*n*-hexylsilane) (PDHS) and poly(methyl(phenyl)silane) (PMPS) incorporated into porous materials MCM-41 and SBA-15, with a pore diameter ranged from 2.8 to 10 nm. Their fluorescence (FL) and excitation spectra were studied at temperatures between 5 and 290 K. The polymer localization in a pore was examined by the x-ray diffraction technique.

The controlled variation of the pore diameter over a wide range (2.8–10 nm) made it possible for the first time to investigate the optical properties of polymers on their change from isolated macromolecules to a film. As will be shown below, this transition depends on the polymer type and occurs via the formation of new spatially independent polymer structures not observed in the spectra of the film. For a thermochromic polymer, as is PDHS, it occurs via the formation of disordered and ordered conformations of polymer chains and clusters. If a polymer is not thermochromic (for example, PMPS) this transition occurs via the formation of separate macromolecules and their clusters.

EXPERIMENTAL PROCEDURE

Silicas MCM-41 and SBA-15 were synthesized by the techniques given in Refs. 6 and 7. The synthesized samples were filtered, washed, and dried in air at 323 K. To remove a template, MCM-41 was first calcinated in an oven for one hour at 373 K (the rate of temperature increase being 1 K/min) and then in dry air at 813 K for 23 hours. The synthesized samples of SBA-15 were first dried at 413 K (the rate of temperature increase being 1 K/min) and then in dry air at 823 K for four hours. The template removal was monitored by the IR spectroscopy method (Specord IR 75). The structures of the calcinated samples were classified by

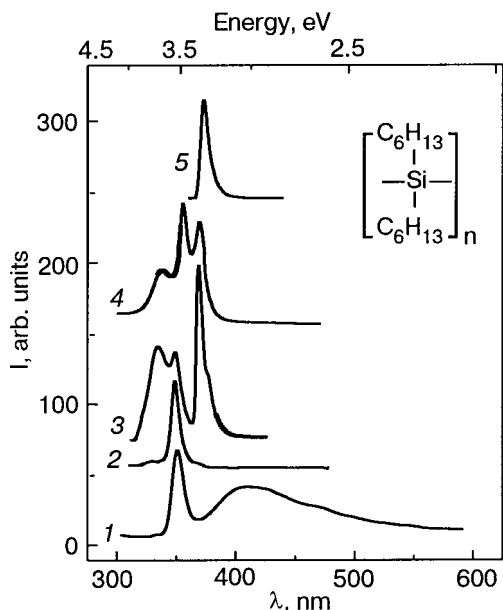


FIG. 1. The fluorescence spectra ($T=5$ K) of PDHS incorporated into nanoporous silicas: 1—of the M165M-41 type, with pore diameter of 2.8 nm, 2-4—of the SBA-15 type, with pore diameter ranging from 5.8, 8, to 10 nm. Curves 2-4 are normalized by the intensity of the band with maximum at 350 nm. Inset: the structural formula of PDHS

using the IR spectroscopy, x-ray diffraction (DRON-3M) and adsorption methods (nitrogen adsorption). Each of MCM-41 and SBA-15 samples displayed intensive Bragg reflections and sharp steps in the isotherms at $p/p_s \sim 0.4$. The isotherms were measured with ASAP 2000 after the samples were degassed at 423 K to 20 Torr for 6 hours. The porous system parameters were calculated from the isotherm absorption branches by the method given in Ref. 8. Polymers PDHS ($M=53600$) and PMPS ($M=11160$) were incorporated into the porous matrix structure from the polymer solutions in toluene (1 wt. %). The sample was mixed with the solution, then the mixture was placed into a dark vessel where it was slowly stirred for some hours at 293 K and kept until the solvent evaporates. The composite obtained was double washed in fresh toluene to remove the polymer from the outer surface. Then the samples were dried for 12 hours at room temperature for the residual moisture to be removed and held within desiccators.

The polymer films were deposited onto a quartz substrate or the surface of a "host" by spin-coating. The FL, phosphorescence, and excitation spectra were taken with DFS-12 and Hitachi MPF-4, integrated with the helium cryostat at temperatures ranging from 5 to 290 K. Fluorescence was excited by light at wavelength 313 nm separated from the emission of a xenon lamp by a monochromator. The absorption spectra ($T=295$ K) of the films and the solutions in toluene (the concentration C being varied from 10^{-7} to 10^{-1} mol/l) were investigated with a spectral-computer system KSVU-23.

EXPERIMENTAL RESULTS

Fluorescence and excitation spectra of nanosized PDHS incorporated into porous silica materials MCM-41 and SBA-15

Figure 1 shows the FL spectra of the nanosized PDHS

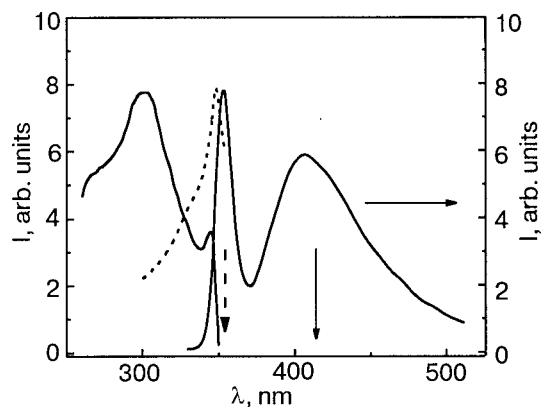


FIG. 2. The fluorescence ($\lambda_{exc}=313$ nm, $T=5$ K) and excitation spectra ($T=5$ K) of composite PDHS/MCM-41 (pore diameter of 2.8 nm). The arrows indicate the FL bands for which the excitation spectra were recorded. The related excitation spectra are shown by corresponding line types.

incorporated into porous materials with different pore diameters: 1—into MCM-41 (the pore diameter of 2.8 nm); 2-4—into SBA-15 with the pore diameter of 5.8, 8, and 10 nm, respectively; 5—the film on quartz ($T=5$ K, $\lambda_{exc}=313$ nm). Curves 1 through 4 are normalized by the band intensity with a maximum at 350 nm. It is known that the FL spectrum of the film ($T=5$ K, $\lambda_{exc}=313$ nm, Fig. 1, curve 5) consists of a narrow band with a maximum at 371 nm which is due to the $\sigma^*-\sigma$ transition in the polymer chain.⁹ In the absorption spectrum of the PDHS film ($T=10$ K) this transition corresponds to an intensive band with a 365 nm maximum. In addition, one can observe a very weak band with a 313 nm maximum that corresponds to the disordered conformation of the polymer chain segments.

As is evident from Fig. 1, the FL spectrum of the PDHS/MCM-41 composite, unlike that of the film on quartz, consists of three bands: a narrow band with a 350 nm maximum which is displaced by 20 nm to a short-wavelength side with respect to the corresponding band in the spectrum of the film, a very weak band with a maximum at 333 nm, and a new wide, intense band in the visible region with a maximum at 410 nm.^{3,4}

The excitation spectrum ($T=5$ K) of PDHS incorporated into porous material MCM-41 with a pore 2.8 nm diameter is shown in Fig. 2. The FL spectrum is illustrated for comparison. As seen from Fig. 2, on recording into the 350 nm FL band (dashed arrow) the excitation spectrum (dashed curve) displays a strong narrow band with a 346 nm maximum and a weak band with a 336 nm maximum. It should be mentioned that the excitation spectrum recorded at $\lambda=410$ nm (solid arrow) exhibits, in addition to the 344 nm band, a new strong band with a maximum at $\lambda=300$ nm (solid curve).

The intensity of the 410 nm, wide FL band decreases substantially with increasing temperature.⁴ At $T=410$ K the spectrum displays only a narrow band, the intensity of which decreases slightly as compared to the considerable reduction of the intensity and broadening of the band observed in the FL spectrum of the film.¹⁰

If PDHS is deposited onto the surface of MCM-41, its FL and excitation spectra will fit the corresponding spectra of the film.

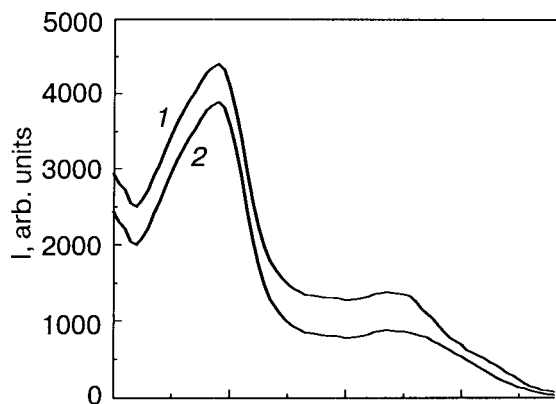


FIG. 3. X-ray powder diffraction patterns for calcined MCM-41 (2.8 nm) (1) and its composite with PDHS polymer (2).

The x-ray powder diffraction patterns for MCM-41 and composite PDHS/MCM-41 are shown in Fig. 3. As can be seen, the intensity of the diffraction peaks for the composite decreases compared to those for pure MCM-41.

The FL spectrum of PDHS incorporated into porous material SBA-15 (pore diameter of 5.8 nm) exhibits no wide band in the visible region, and the same is true for the excitation spectrum. Aside from the 333 nm and 350 nm bands (Fig. 1, curve 2), the spectrum also displays a very weak long-wavelength band with a maximum at 367 nm. With increasing pore diameter up to 8 nm the FL spectrum displays the same bands, but they are shifted to longer wavelengths and their intensities show a considerable redistribution: the intensities of the 335 and 368 nm bands increase considerably (Fig. 1, curve 3).

The FL spectrum of PDHS incorporated into SBA-15 with the pore diameter of 10 nm displays at once the same three bands shifted to the red side (Fig. 1, curve 4). The greatest shift is observed for the central band. The existence of the three bands is supported in studies of the excitation spectra of this composite at $T=5$ K (Fig. 4). As seen from Fig. 4, to the FL bands with the 337, 335, and 369 nm maxima (dashed, dotted, and solid arrows, respectively) correspond the excitation bands with the 318 nm, 345 nm, and

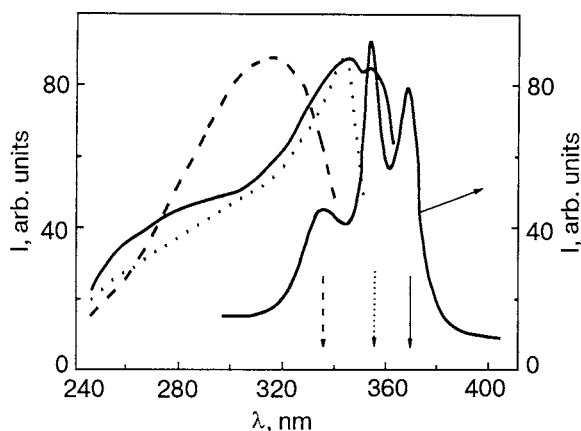


FIG. 4. The fluorescence ($\lambda_{exc}=313$ nm, $T=5$ K) and excitation spectra ($T=5$ K) of composite PDHS/SBA-15 (pore diameter of 10 nm). The arrows indicate the FL bands for which the excitation spectra were recorded. The related excitation spectra are shown by corresponding line types.

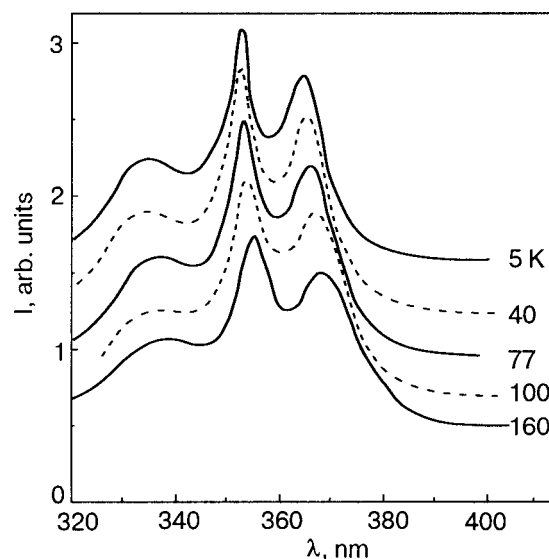


FIG. 5. Temperature dependence of FL spectra PDHS/SBA-15 composite (pore diameter of 10 nm, $\lambda_{exc}=313$ nm).

357 nm peaks (dashed, dotted, and solid curves), respectively.

It should be noted that only on recording the 369 nm FL band can one observe the 345 nm band in addition to the 357 nm band in the excitation spectrum. Decomposition of the FL spectra into three curves demonstrated that the half-width of the short-wavelength band is much broader than those of the two longer-wavelength bands (16, 9, 10 nm, respectively). The experiment showed (Fig. 5) that the intensity of the FL band of PDHS/SBA-15 composites was practically independent of temperature, as opposed to the red shift and strong broadening of the FL band with increasing temperature for a bulk film of PDHS on a quartz substrate.¹⁰

Fluorescence and excitation spectra of PMPS incorporated into porous silica materials MCM-41 and SBA-15

It is known¹¹ that the FL spectrum of the PMPS film on a quartz substrate ($T=5$ K, $\lambda_{exc}=313$ nm) consists of two bands: a narrow band with maximum at 352 nm which is associated with the $\sigma^*-\sigma$ transitions in the polymer chain, and a wide band in the visible region with a maximum at 410 nm and an extended long-wavelength edge up to 550 nm (Fig. 6, curve 1). The latter is responsible for by the transitions of the polymer chain to defect states.¹² The absorption spectrum of the PMPS film on quartz ($T=5$ K) consists of two bands with maxima at 338 and 270 nm, which are associated with the $\sigma^*-\sigma$ transitions in the main polymer chain and in the phenyl ring. Similar bands are observed in the excitation spectrum of this film ($T=5$ K) on recording into the FL band with $\lambda_r=352$ nm. For $\lambda_r=410$ nm one can observe an additional band with a maximum at 305 nm.

Illustrated in Fig. 6 are the FL spectra ($T=5$ K, $\lambda_{exc}=313$ nm) of the PMPS film on quartz (curve 1) and of nano-sized PMPS incorporated into porous material with different pore diameters: curve 2—into MCM-41 (the pore diameter of 2.8 nm); curves 3–5—into SBA-15 with pore diameter of 5.8, 8, and 10 nm, respectively. Curve 2 in Fig. 6 indicates that the FL spectrum of PMPS incorporated into MCM-41 (a pore 2.8 nm diameter) consists of two bands: a weak, narrow

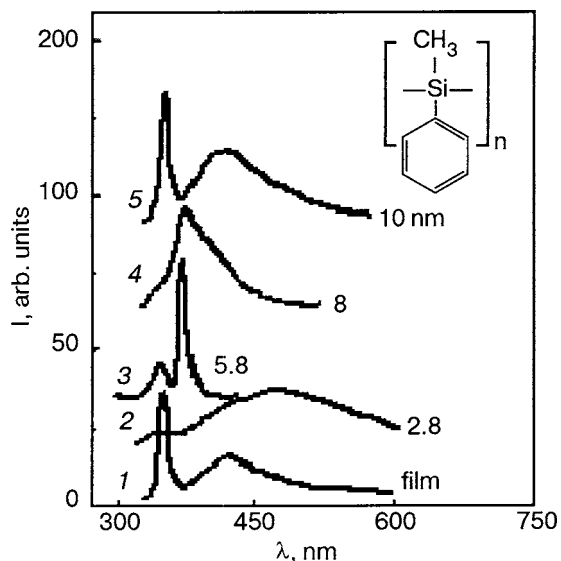


FIG. 6. FL spectra ($T=5$ K) of PMPS incorporated into nanoporous silicas: 1—of the M165M-41 with pore diameter of 2.8 nm, 2-4—of the SBA-15 with pore diameter ranging from 5.8, 8, to 10 nm. Curves 2-4 are normalized by the intensity of the band with maximum at 350 nm. Inset: the structural formula of PMPS.

band with a maximum at 345 nm and a very intensive, wide band with a maximum at 470 nm. The narrow band maximum is shifted relative to that in the FL spectrum of the film (Fig. 6, curve 1) to the short-wavelength side by 7 nm. As the temperature is increased from 5 to 290 K the wide band intensity decreases and its maximum shifts towards a red side (Fig. 7). The intensity of the narrow $\sigma^*-\sigma$ band is little affected. As is evident from Fig. 8, the excitation spectrum of this sample ($T=5$ K) displayed, on recording into the 345 nm FL band (dashed arrow), the following bands: a 334 nm band and a very weak band in the vicinity of 270 nm; moreover, at $\lambda_r=470$ nm (solid arrow) one can observe one more band with a maximum at 301 nm (solid curve).

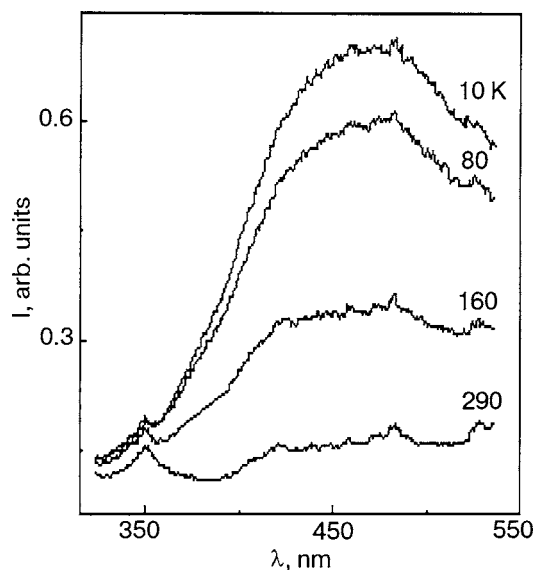


FIG. 7. Temperature dependence of the FL spectra of PMPS/MCM-41 composite (pore diameter of 2.8 nm, $\lambda_{exc}=313$ nm).

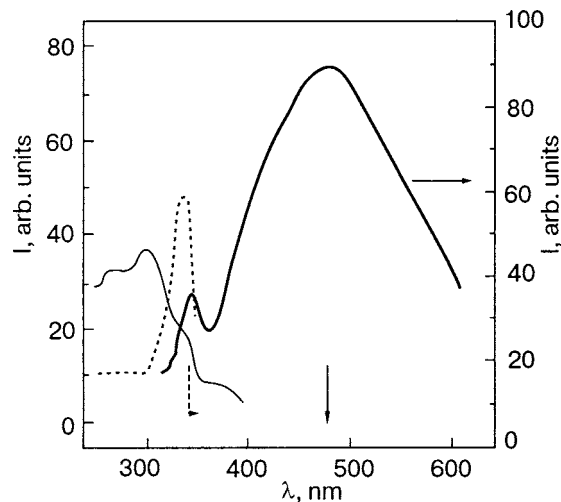


FIG. 8. FL ($\lambda_{exc}=313$ nm, $T=5$ K) and excitation spectra ($T=5$ K) of composite PMPS/MCM-41 (pore diameter of 2.8 nm). The arrows indicate the FL bands for which the excitation spectra were recorded. The related excitation spectra are shown by corresponding line types.

It should be mentioned that the FL and excitation spectra of the polymer deposited on the porous material surface are coincident with those of the film. The FL spectrum of PMPS incorporated into the porous silica materials with a 5.8 nm pore diameter is shown in Fig. 6 (curve 3). The spectrum displays a weak band whose maximum is coincident with that of the band for the composite PMPS/MCM-41. This band has a long-wavelength shoulder with a 352 nm maximum. Of important fact is the disappearance of not only the wide FL band in the visible region with maximum at 470 nm that was observed in the FL spectrum of the PMPS/MCM-41 composite, but also of the band with maximum at 410 nm observed in the FL spectrum of the film. Of importance also is the emergence of a new narrow, intense band with a 372 nm maximum in the FL spectrum of this composite. The excitation spectrum of this sample ($T=5$ K, $\lambda_r=345$ nm, Fig. 8) demonstrates a single wide band with a 326 nm maximum. At $\lambda_r=352$ nm the maximum is shifted towards 338 nm and at $\lambda_r=372$ nm to 343 nm. What is more, in the latter case there appears a band with a 302 nm maximum.

The FL spectrum of the composite PMPS/SBA-15 (pores 8 nm diameter, $T=5$ K, $\lambda_{exc}=313$ nm) demonstrates no narrow band with the 345 nm maximum, while one can observe a strong narrow band with a 374 nm maximum, a weak short-wavelength shoulder with a 355 nm maximum, and a strong long-wavelength shoulder with a 392 nm maximum (Fig. 6, curve 4). The excitation spectrum of this composite, on recording into the 355 nm FL band (solid arrow), displays a 260 nm band (not shown in the figure), a 290 nm strong band, a weak 329 nm band, and a very weak 342 nm band (Fig. 9). It is of interest that on recording into the 374 and 392 nm bands (dotted and dashed curves, respectively) one can observe the same bands but of different intensities.

The FL (Fig. 6, curve 5) and excitation spectra of PMPS/SBA-15 (pores 10 nm diameter) are coincident with the corresponding spectra of the film.

It should be noted that porous silica materials MCM-41 and SBA-15 do not fluorescence at 5 K; one can observe only phosphorescence in the 400–500 nm region, therefore

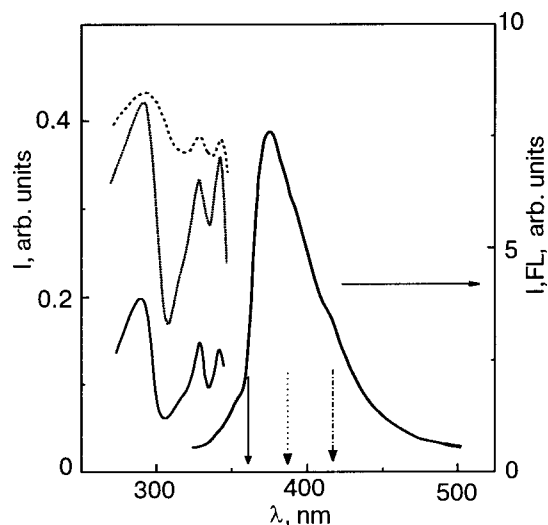


FIG. 9. FL ($\lambda_{exc}=313$ nm, $T=5$ K) and excitation spectra ($T=5$ K) of composite PMPS/SBA-15 (pore diameter of 8 nm). The arrows indicate the FL bands for which the excitation spectra were recorded. The related excitation spectra are shown by corresponding line types.

the process of excitation energy transfer from the polymer to the porous material can be assumed not to occur. The absorption spectrum of these materials consists of a wide band with a maximum at about 250 nm.

FL and absorption spectra of PDHS and PMPS solutions

The FL spectra of PDHS solid solutions in toluene are studied with increasing polymer concentration C from 10^{-7} to 10^{-2} mol/l [Fig. 10, curves 1-4: 1— 10^{-7} ; 2— 10^{-5} ; 3— 10^{-4} and 4— 10^{-2} mol/l ($T=10$ K, $\lambda_{exc}=313$ nm)]. As seen from Fig. 10, curve 1, the FL spectrum at very low concentrations displays a single band with maximum at 358 nm which presumably corresponds to the transition from one polymer chain. As the polymer concentration is increased there appear new bands, the maxima of which are shifted to the red side relative to the isolated polymer chain: 362, 369, and 375 nm. At $C=10^{-7}$ mol/l the absorption

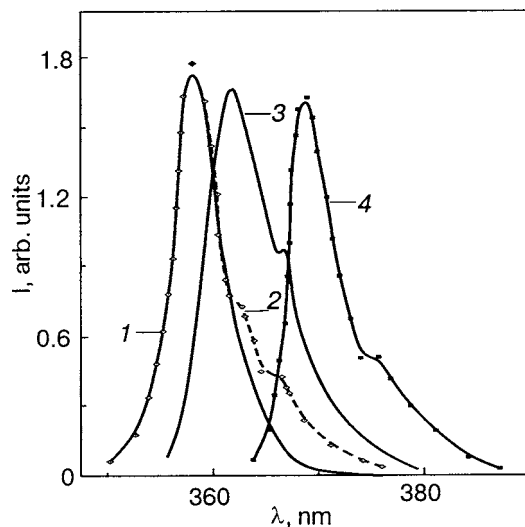


FIG. 10. Concentration dependence of FL spectra of PDHS solution in toluene at 10 K at different concentrations C [mol/l]: 10^{-7} (1), 10^{-5} (2), 10^{-4} (3), and 10^{-2} (4).

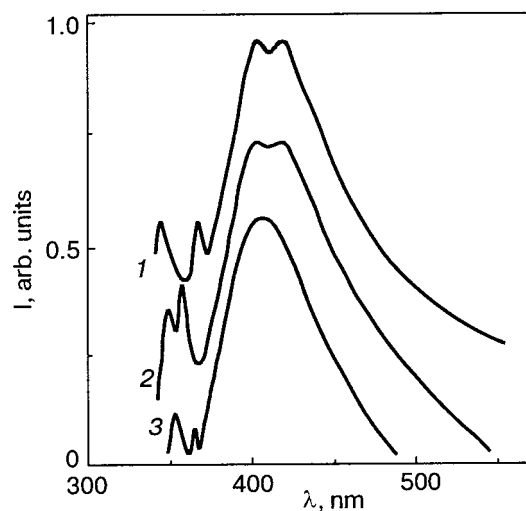


FIG. 11. Concentration dependence of FL spectra of PMPS solution in toluene at 10 K different concentrations C [mol/l]: 10^{-6} (1), 10^{-4} (2), and 10^{-1} (3).

spectrum demonstrates only one band with a maximum at 317 nm, but at $C=10^{-2}$ mol/l there appears an additional weak band with a maximum which is close to that of the band in the absorption spectrum of the polymer film.

The appearance of new longer-wavelength bands in the FL spectrum of PDHS solid solutions with increasing the polymer concentration suggests that there occur clusters consisting of different numbers of polymer chains, the number of chains increasing with C .

The absorption (295 K) and FL ($T=10$ K, $\lambda_{exc}=313$ nm) spectra of the PMPS solution in toluene were studied with C varying from 10^{-7} to 10^{-1} mol/l. The absorption spectra of the diluted solutions are found to involve two bands with maxima at 280 and 326 nm, and at $C=10^{-4}$ mol/l the spectra of the solution and the film are coincident. It is known that the FL spectrum of the PMPS solution is independent of C .¹¹ But we have found that the FL of the PMPS solution in toluene depends essentially on C . The FL spectrum of the PMPS solution with C varying from 10^{-6} to 10^{-1} mol/l is shown in Fig. 11. As is evident, at $C=10^{-6}$ mol/l the narrow band is split into two components of same intensity with maxima at 344 and 366 nm (curve 1). The same is true of the wide band: it is split into 403 and 418 nm components. As the concentration is increased, there occurs a considerable change in the positions of the narrow-band components—these occur at 348 and 356 nm, while the wide-band components are little affected (curve 2). As $C=10^{-1}$ mol/l the narrow-band components are shifted towards the red side and become 352 and 364 nm, respectively (the longer-wavelength band intensity is much lower). In this case the wide band is no longer split and has a maximum at 405 nm (curve 3). It should be emphasized that at the above C the short-wavelength band maximum is coincident with the maximum of the corresponding band in the spectrum of the film. It seems likely that in the solution there are two spatially independent fluorescence centers which correspond to the polymer chains with different distribution of short and long segments over length. Similar doublets with maxima at 350 and 358 nm were observed in the FL spectra of thick ($d \geq 7$ nm) PMPS films.³

DISCUSSION

The controlled variation in pore diameter from 2.8 to 10 nm made it possible to study for the first time the optical properties of polymers at their transition from isolated macromolecules to a film. Such a transition is shown to depend on polymer type and occurs through the formation of new spatially independent polymer structures not observed in the spectra of the film.

Let us consider the results of the investigation of the optical spectra of composites in the case where the polymers in question are incorporated into small pores of MCM-41 (pores 2.8 nm diameter). It follows from the relationship of sizes between a single chain of a macromolecule and a pore (1.6 nm for PDHS and ~ 0.97 nm for PMPS) that in a separate pore of MCM-41 there are only one macromolecule of PDHS and two macromolecules of PMPS. In that case the intermolecular interaction between macromolecules is non-existent or considerably decreased for PDHS and PMPS, respectively. So the $\sigma^* - \sigma$ transition should be shifted towards the blue side with respect to that in the film, and its position should be close to the electronic transition in the dilute solution, as observed experimentally.⁴ As is evident from our studies, this shift is 20 nm for PDHS (Fig. 1, curve 1) and 7 nm for PMPS (Fig. 6, curve 2). Moreover, the FL band maximum is at 358 nm for the dilute PDHS-toluene solution ($T=10$ K) and at 348 nm for PMPS (Fig. 11, curve 2), which is close to the FL band maximum in the composites.

Localization of polymers in pores is supported by the x-ray diffraction data for MCM-41 and the composite PDHS/MCM-41. It is known¹⁴ that the intensity of diffraction peaks decreases as compared to that for pure MCM-41. Such dependences were found for the PDHS/MCM-41 composites (Fig. 3), evidence in favor of the existence of the polymer macromolecules in a pore.

It should be emphasized that the FL spectrum of the polymers incorporated into a pore 2.8 nm diameter differs essentially from that of the solutions. Indeed, the FL spectrum of the composites exhibits extra wide bands in the visible spectral region with maxima of 410 nm (Fig. 1, curve 1) and 470 nm (Fig. 6, curve 2) for PDHS/MCM-41 and PMPS/MCM-41, respectively. These bands are not observed in the FL spectra of the films.

It is known that the electronic transition position of these polymers depends highly on polymer chain conformation. The conformation modification may give rise to defects in the polymer chain, i.e., new bands in the FL spectrum. We suggest that the new wide FL bands in the visible region with maxima 410 and 470 nm for PDHS and PMPS, respectively (Fig. 1, curve 1 and Fig. 6, curve 2), which are not observed in the spectra of the films and polymer solutions, are of a defect nature and associated with the conformation modification of some segments of the polymer chain caused by the interaction with SiOH groups on the pore surface.⁵ This suggestion is supported by the following facts:

1. The lack of the wide band with a 410 nm maximum in the FL spectrum of PDHS incorporated into MCM-41, with a high hydrophobic behavior.⁵
2. The appearance of a new band in the excitation spectrum of PDHS incorporated into a pore 2.8 nm diameter on

excitation into a wide FL band with a 410 nm maximum which is associated with the change in the environment symmetry near defects and the allowing of the symmetry-forbidden transition $^1A_g - ^1A_g$ (Ref. 15).

3. A considerable decrease in the wide FL band intensity with increasing temperature from 5 to 290 K. It is conceivable that the motion of polymer fragments becomes feasible with increasing temperature, resulting in reduction of polymer chain-pore surface interaction and modification of conformation of polymer chains near the surface.

Hence, we may suggest that a part of the polymer chain oriented relative to the surface will give a narrow FL band while the defective part of the chain near the pore surface provides a broad band, as observed experimentally.

The FL spectrum of PDHS incorporated into SBA-15 (Fig. 1, curves 2-4) differs essentially from the FL spectrum of the PDHS/MCM-41 composite: it lacks the wide FL band associated with the transition from defect states that come into existence due to the modification of the polymer chain conformation in a limited volume; the spectrum acquires structure in the UV region and even displays three bands. In addition, as the pore diameter increases one can observe a substantial redistribution of intensity among these bands, namely, the intensities of shorter- and longer-wavelength bands increase and the maxima of all bands are shifted by some nanometers towards the red side. It is of interest that these three FL bands exist simultaneously. This suggests that these bands correspond to spatially independent states, the energy transfer between which is much reduced.

The above peculiarities in the FL and excitation spectra of composite PDHS/SBA-15 are in correlation with the increase of the number of macromolecules in a pore. Now the macromolecules will be oriented not only relative to the pore surface but relative to each other as well. In that case the polymer-surface interaction will diminish and the polymer-polymer interaction will increase, resulting in the disappearance of the wide FL bands in the visible region (an additional verification of their nature) and the appearance of new bands in the UV region. The longest-wavelength band is suggested to be associated with the formation of clusters. In correlation with this is the good coincidence of the maximum of this band with the corresponding band in the FL spectrum of the concentrated PDHS-toluene solution (Fig. 10, curve 4) and with the FL maximum of the film (Fig. 1, curve 5). Interaction between oriented chains in a cluster is supposed to cause a stabilization of their structure and to give rise to a great number of long segments in the polymer chain. In agreement with this is the fact that it is precisely the 355 and 369 nm bands associated with transitions in separated polymer chains and clusters that are the narrowest bands in the spectra.

Orienting the polymer chains causes the number of chains with different conformations to reduce, resulting in a decrease of inhomogeneous broadening and increase of energy migration efficiency as compared to the film, as evidenced by the weak temperature dependence of the FL bands intensity for the composites under consideration (Figs. 5 and 7).

Observation of the shortest-wavelength 337 nm band suggests that there are short chain segments in a pore which

are of more disordered conformation. In agreement with this is the fact that the half-width of this band is the widest both in the FL spectrum and in the excitation spectrum. We suggest that the disordered polymer chains are near the pore surface, where the interaction with that surface is more important. Additional evidence supporting this suggestion is the fact that this band is absent in the spectrum of the solutions. It should be mentioned that a similar FL band was observed in Ref. 16 for thin PDHS films on quartz substrates with decreasing film thickness down to 7 nm. It was shown that in that case the polymer chain had a gauche conformation, and the respective broadening of the short-wavelength FL band occurred.

The FL spectrum of composite PMPS/SBA-15 displays only two bands in the UV spectrum with varying pore diameter from 5.8 to 10 nm (Fig. 6, curves 3-5). These are associated with the transitions from isolated macromolecules and their clusters. The latest is supported by the coincidence of the band maximum with that in the FL spectrum of the film. This distinction compared the corresponding spectra of PDHS/SBA-15 may be due to the fact that unlike PMPS, PDHS is a thermochromic polymer.

The most essential distinctions in the FL spectrum of PMPS/SBA-15 as compared to that of PMPS/MCM-41 are associated with the changes in the visible FL region. There is the disappearance not only of the 470 nm defect FL band which is due to the modification of the polymer chain segment conformation but also of the 420 nm defect band which is observed in the FL spectrum of the film. The surprising thing is that there appears a new strong, narrow band with a maximum at 372 nm (Fig. 6, curve 3). As the pore diameter increases, the band becomes wider and transforms gradually into a wide band with a 420 nm maximum (Fig. 6, curves 4, 5), suggesting its defect nature. It seems likely that the separation of polymer chains of a certain conformation type is connected with their orientation in a pore. Gaining a more complete understanding of the band nature requires further investigation.

It should be noted that papers^{17,18} have pointed to the relationship between the occurrences of isolated polymer chains or their aggregates in nanopores as well as of polymer chains with amorphous or crystal packing and the organic polymer type and pore diameter.

CONCLUSIONS

The FL and excitation spectra of silicon-organic polymers PDHS and PMPS incorporated into nanopores of porous silica materials MCM-41 and SBA-15 have been studied with varying pore diameter from 2.8 to 10 nm. It is shown that the optical spectra of the nanosized polymers in a limited pore volume differ essentially from those of films and solutions of the polymers and depend on nanopore size. For a pore of a small diameter (2.8 nm) one can observe mainly separated macromolecules whose properties are determined by the polymer-pore surface interaction. The appearance of new wide bands in the visible region of the spectra of these polymers which are of defect nature is associated with a considerable modification of the polymer chain conformation due to the interaction with SiOH groups on the

pore surface. In this case the forbidden transition is allowed, resulting in a change of the environment symmetry near such defects.

As the pore diameter increases, a number of polymer chains in a pore increase and the intermolecular interaction between macromolecules becomes significant. It is shown that the FL and excitation spectra of such composites are structural in the UV region and differ essentially from those in the case where there is an isolated macromolecule in a pore. It is found that transition from an isolated macromolecule to a film in a limited volume depends on polymer type and occurs through the formation of disordered and ordered conformations of polymer chains and their clusters. It should be mentioned that in the FL spectrum of PMPS/SBA-15 there appears a new narrow band with a maximum at 372 nm instead of a wide band with a 410 nm maximum. Such a considerable narrowing of the visible FL band (almost by a factor of seven) was observed for the first time in the spectrum of nanosized polymers, and further investigation is required to explain this fact.

It is of interest that the FL spectrum of composite PMPS/SBA-15 (pore 10 nm diameter, 10 macromolecules in a pore) is coincident with the spectrum of the polymer film.

We gratefully acknowledge Dr. G. Telbiz for preparation of the specimens used.

The work was partially supported by the Ministry of Education and Science, Grant No. M/128-2005.

^aE-mail: ostap@iop.kiev.ua

- ¹H. Suzuki, H. Meyer, S. Hoshino, and D. Haarer, *J. Appl. Phys.* **78**, 2684 (1995).
- ²M. Wuchse, S. Tasch, G. Leising, F. Lunzer, and G. Marschner, *Croat. Chem. Acta* **74**, 867 (2001).
- ³N. Ostapenko, G. Telbiz, V. Ilyin, S. Suto, and A. Watanabe, *Chem. Phys. Lett.* **383**, 456 (2004).
- ⁴N. Ostapenko, N. Kotova, G. Telbiz, S. Suto, and A. Watanabe, *Fiz. Nizk. Temp.* **30**, 658 (2004) [*Low Temp. Phys.* **30**, 494 (2004)].
- ⁵N. Ostapenko, N. Kotova, V. Lukashenko, G. Telbiz, V. Gerda, S. Suto, and A. Watanabe, *J. Lumin.* **112**, 381 (2005).
- ⁶C. T. Kresge, M. E. Leonowicz, W. J. Roth, J. C. Vartuli, and J. S. Beck, *Nature (London)* **359**, 710 (1992).
- ⁷D. Zhao, Q. Huo, J. Feng, B. F. Chmelka, and G. D. Stucky, *J. Am. Chem. Soc.* **120**, 6024 (1998).
- ⁸E. P. Barrett, L. G. Joyner, and P. P. Halenda, *JACS* **73**, 373 (1951).
- ⁹S. Suto, M. Shimizu, T. Goto, A. Watanabe, and M. Matsuda, *J. Lumin.* **76-77**, 486 (1998).
- ¹⁰M. Shimizu, S. Suto, T. Goto, A. Watanabe, and V. Matzuda, *Phys. Rev. B* **63**, 073403 (2001).
- ¹¹O. Ito, M. Terajima, T. Azumi, N. Matsumoto, K. Takeda, and M. Fujino, *Macromolecules* **22**, 1718 (1989).
- ¹²S. Toyoda and M. Fujiki, *Chem. Phys. Lett.* **293**, 38 (1998).
- ¹³Yu. A. Skryshevski, *Fiz. Tverd. Tela (Leningrad)* **44**, 1705 (2002) [*Phys. Solid State* **44**, 1785 (2002)].
- ¹⁴B. Marler, U. Oberhagemann, S. Vortmann, and H. Gies, *Microporous Mater.* **6**, 375 (1996).
- ¹⁵R. G. Kepler and Z. G. Soos, *Phys. Rev. B* **43**, 11908 (1991).
- ¹⁶M. M. Despotopoulou, R. D. Miller, J. F. Rabolt, and C. W. Frank, *J. Polym. Sci., Part B: Polym. Phys.* **34**, 2335 (1996).
- ¹⁷M. Okazaki, K. Toriyama, and S. Anandan, *Chem. Phys. Lett.* **401**, 363 (2005).
- ¹⁸A. J. Cadby and S. H. Tolbert, *J. Phys. Chem.* **109**, 17879 (2005).